

Stationary and Oscillatory Onsets of Surface Tension Gradient-Driven Convection in Two-Layer Systems

Leonardo S. de B. Alves

leoalves@seas.ucla.edu

Robert E. Kelly

rekhome@ucla.edu

Mechanical and Aerospace Engineering Department,
School of Engineering and Applied Science,
University of California at Los Angeles,
PO Box 951597, 48-121 Engr Bldg, Los Angeles, CA 90095-1597, USA.

Abstract. *The flow field generated by temperature gradient induced density variations is one of the most well known problems in natural convection. In such cases, buoyancy is the main mechanism responsible for triggering the instability that drives the flow. However, there are two important exceptions: microgravity and microscale fluid systems. Under any of these conditions, the surface tension gradients that appear at the interface between different fluids become increasingly important. In this work we examine monotonic and oscillatory instabilities induced by surface tension gradients by means of a linear stability analysis in a two-layer system with finite depths. Interfacial deformation is included and gravity is considered to act at the interface, although buoyancy forces are ignored within the fluid layers. First, prescribed temperature boundary conditions are imposed at the top and bottom rigid surfaces. However, results are also obtained for the case of a prescribed heat flux imposed at the bottom surface. Our study is focussed on obtaining estimates for the critical depth ratios at which discontinuous character of the neutral curves for monotonic instability occurs. We also show that the onset of convection may be oscillatory rather than monotonic depending on the depth ratio value.*

keywords: *Linear Stability Analysis, Marangoni Convection, Symbolic Computation*

1. Introduction

Thermocapillary convection arises from the fluid stress induced by a gradient of surface tension along a fluid interface or surface when this gradient is associated with varying temperature. Solutalcapillary convection, associated with a solute gradient, gives rise to similar phenomena. An interesting and complete summary of the origins of this research topic is given in the preface of Nepomnyashchy et al., 2001. Many of the early observations had to do with solutal effects. However, thermocapillary convection has been investigated extensively since the experimental study of Block, 1956 and the theoretical study of Pearson, 1958. These studies led to the conclusion that the convection observed by Bénard, 1900 in thin, heated liquid films was apparently due to thermocapillary rather than buoyancy effects. The recently published books of Nepomnyashchy et al., 2001 and Colinet et al., 2001 present a broad survey of the field, whereas the book by Narayanan and Schwabe, 2003 provides a survey of recent research topics. These books contain a discussion of the different types of application of the thermocapillary convection results. Many of these occur in technology, which is not surprising in view of the common occurrence of fluid interfaces in material processing, chemical and biomedical engineering. Specific applications in material processing are summarized in the proceedings of a conference organized by the Royal Society of London (Hondros et al., 1998). Of special interest in this area is the growth of single crystals (Kuhlmann, 1999), which has been emphasized in NASA's program on materials processing in space. Due to the diminished role of buoyancy, a microgravity (space) environment is ideally suited for the investigation of thermocapillary phenomena. For instance, Simanovskii et al., 2003 present the results of an experiment done in space on Bénard-Marangoni convection in a three-fluid system.

The present work considers the dynamics of two distinct immiscible fluid layers constrained by parallel horizontal solid walls. The interface between these two fluids is allowed to deform. Although we assume negligible buoyancy forces within the fluids, the effect of gravity in deforming the interface is also included. The mathematical model we use follows the one used by Jiménez-Fernández and García-Sanz, 1996, where both solid walls were maintained at constant temperature. We extended this model to allow a constant heat flux at

the lower wall. One of the main reasons for doing so is the recognition by Slavtchev et al., 1998 that oscillatory instability can occur with a constant heat flux condition for situations where oscillations are not predicted with a constant temperature condition. Another important reason is that stabilization of Rayleigh-Bénard-Marangoni convection via feedback control (Or and Kelly, 2001) is simplest to realize experimentally by controlling the heat flux instead of the temperature at the lower wall.

The Bénard-Marangoni instability of a gas-liquid system has been studied in the past by many authors (Yang, 1992; Zaman and Narayanan, 1996; Pérez-García et al., 1998), including Takashima, whose work focussed on both stationary (Takashima, 1981a) and oscillatory (Takashima, 1981b) onset of convection. However, the dynamics of the gas layer was disregarded in these previous studies. The limiting conditions, in terms of lower and upper bounds for the depth ratio between the two layers (Simanovskii and Nepomnyashchy, 1993), that must be satisfied in order for these one-layer results to be valid are discussed in the present paper, where special focus is placed on the long wavelength instability for mean heat transfer in either direction. Results are also obtained for the case of two liquid layers.

One of the difficulties in the study of the current problem comes from the great number of parameters present in most models and their proper usage. Velarde et al., 2001 pointed out that some of the published results were not consistent with the mathematical model used and that these inconsistencies were related to the Boussinesq approximation. This was also pointed out by Regnier et al., 2000, who added that some reported results were unrealistic from the experimental point of view because the Crispation and Bond numbers chosen lead to fluid thicknesses too small to be attained in experiments on earth. These requirements lead to constraints of small temperature differences and small fluid depths in order to maintain small Rayleigh numbers in both fluids and hence justify the absence of buoyancy forces.

2. Mathematical Model

The present model is based on the work of Jiménez-Fernández and García-Sanz, 1996, and its notation and scaling is the same as used by Johnson and Narayanan, 1999 and Colinet et al., 2001. The model consists of two infinite horizontal fluid layers bounded above, at $z = d_2$, by a rigid surface maintained at a constant temperature T_2 and below, at $z = -d_1$, by another rigid surface maintained at either a constant temperature T_1 or a constant heat flux q_s . The undisturbed interface is located at $z = 0$ and the interfacial surface tension $\sigma(T)$ is assumed to linearly decrease with increasing temperature as $\sigma(T) = \sigma_0 - \sigma_T(T - T_0)$, where T_0 is the temperature of the interface at rest. All the other physical properties are taken to be constant and are defined as: dynamic and kinematic viscosities μ_i and ν_i , thermal conductivities and diffusivities k_i and κ_i , and densities ρ_i , where the index $i = 1$ refers to the lower layer and the index $i = 2$ to the upper layer. The absence of an index indicates a property ratio (ex: $\mu = \mu_2/\mu_1$). The problem is written in dimensionless form by introducing the following scales: length d_1 , time d_1^2/κ_1 , velocity κ_1/d_1 and temperature $\Delta T = T_1 - T_0$ (or $q_s d_1/k_1$).

The dimensionless parameters that appear are: depth ratio $d = d_2/d_1$, Prandtl number $Pr = \nu_1/\kappa_1$, complex frequency λ , overall wavenumber $\alpha = d_1(\alpha_x^2 + \alpha_y^2)^{1/2}$, Crispation number $Cr = \mu_1\kappa_1/\sigma_0 d_1$, Bond number $Bo = g d_1^2(\rho_1 - \rho_2)/\sigma_0$ and the Marangoni number $Ma = \sigma_T d_1^2 \beta/\mu_1\kappa_1$, where β is the temperature gradient across the lower layer and is equal to either $\Delta T/d_1$ for a prescribed temperature at the lower wall or q_s/k_1 for a prescribed heat flux there. The Crispation number accounts for the magnitude of the interface deformation whereas the Bond number quantifies the capillarity equilibrium between gravity and surface tension forces.

The solution of the linear eigenvalue problem, where the real part of λ is set to zero, yields the critical Marangoni number. The onset of convection will be stationary (oscillatory) if the complex part of λ is set to zero (nonzero). When the onset of convection is oscillatory, the frequency of oscillation (complex part of λ) is obtained by requiring the imaginary part of the critical Marangoni number to be zero. Further details about the mathematical model used here can be found in the previously mentioned references.

3. Linear Stability Analysis

The solution for the marginal Marangoni number for the case of a stationary onset of convection where both horizontal walls have prescribed temperatures was obtained by Smith, 1966. His analytical solutions was first reproduced through a symbolic computation procedure developed using the *Mathematica* system (Wolfram, 1999). This procedure was generalized in such a way that allowed us to simply replace the prescribed temperature boundary condition at the lower surface by a prescribed heat flux condition and run once again the code in order to generate the following new analytical solution:

$$Ma = \left(2\alpha^2(Bo + \alpha^2)\kappa csch(\alpha) \left(k \cosh(\alpha) \cosh(d\alpha) + \sinh(\alpha) \sinh(d\alpha) \right) \left(4\alpha \left(1 + d(\mu + 2\alpha^2(d + \mu)) - d\mu \cosh(2\alpha) - \cosh(2d\alpha) \right) - (2 + 4d^2\alpha^2) \sinh(2\alpha) + (1 - \mu) \sinh(2(1 - d)\alpha) - 2(\mu + 2\alpha^2\mu) \sinh(2d\alpha) + (1 + \mu) \sinh(2(1 + d)\alpha) \right) \right) / \left(d^3\alpha^3 (Bo + \alpha^2) (\cosh(2\alpha) - 1 - 2\alpha^2) \cosh(d\alpha)^3 \right)$$

$$\begin{aligned} & \coth(\alpha) + 4 Cr \alpha^5 \kappa \cosh(3 d \alpha) \coth(\alpha) + \alpha^3 \cosh(d \alpha) \coth(\alpha) \left(4 Cr \alpha^2 \kappa (-1 + 2 d^2 (2 \alpha^2 (\mu - 1) \right. \\ & + \mu) - 2 d^2 \mu \cosh(2 \alpha)) + d^3 (Bo + \alpha^2) (1 + 2 \alpha^2 - \cosh(2 \alpha)) \sinh(d \alpha)^2 \Big) + \sinh(d \alpha) \left(\alpha (2 + \alpha^2) \right. \\ & (Bo + \alpha^2) (1 + 2 d^2 \alpha^2) \kappa + 8 Cr \alpha^5 \kappa (d^2 (2 \alpha^2 (\mu - 1) + \mu) - 1) - 8 Cr d^2 \alpha^5 \kappa \mu \cosh(2 \alpha) + \alpha \kappa \\ & \left. \left((8 Cr - 1) \alpha^4 - (2 + Bo) \alpha^2 - 2 Bo \right) \cosh(2 d \alpha) - \kappa (Bo + \alpha^2) (\cosh(2 \alpha) - 1 + 2 \alpha^2) \coth(\alpha) \right. \\ & \left. \left. (1 + 2 d^2 \alpha^2 - \cosh(2 d \alpha)) / 2 + (Bo + \alpha^2) (1 + 2 \alpha^2 - \cosh(2 \alpha)) \coth(\alpha) \sinh(d \alpha)^2 \right) \right) . \end{aligned} \quad (1)$$

An analytic expression for the marginal Marangoni number at zero wavenumber can be obtained from Smith, 1966 for the prescribed temperature case and is given by

$$Ma(0) = \frac{2 Bo d (d + k) (d + \mu)}{3 Cr (1 + d) (d^2 - \mu)} . \quad (2)$$

The same is done with solution (1) for the prescribed heat flux case, and we obtain

$$Ma(0) = \frac{2 Bo d k (d + \mu)}{3 Cr (d^2 - \mu)} . \quad (3)$$

In both limiting cases (2) and (3) there is a critical depth ratio given by $d_{c1} = \sqrt{\mu}$ at which the zero wavenumber Marangoni number changes sign discontinuously. Although Smith, 1966 did not comment upon this fact when looking at the prescribed temperature case, Simanovskii and Nepomnyashchy, 1993 gave a detailed account of it in their book. This discontinuous behavior appears for any choice of fluids, and obviously cannot be predicted by any model that neglects the dynamics of the gas layer in, for instance, an air-water system.

We note that relations (2) and (3) differ by a factor $(1 + dk^{-1})/(1 + d)$, which tends to k^{-1} in the limit $d \rightarrow \infty$ and to 1 in the limit $d \rightarrow 0$. Hence, the large wavelength results are more sensitive to the thermal boundary condition at the lower wall for the case of large depth ratios.

One is also able to extend results (2) and (3) to find out how the marginal Marangoni number behaves as it approaches the zero wavenumber limit. For the prescribed temperature case, the $O(\alpha^2)$ approximate expression obtained by Simanovskii and Nepomnyashchy, 1993 is

$$Ma \simeq \frac{240 d \kappa (Bo + \alpha^2) (d + k) (d + \mu)}{360 Cr \kappa (1 + d) (d^2 - \mu) + 3 \alpha^2 Bo d^3 (\kappa - d^2)} , \quad (4)$$

whereas for the prescribed heat flux case, our $O(\alpha^2)$ approximate expression is given by

$$Ma \simeq \frac{240 d k \kappa (Bo + \alpha^2) (d + \mu)}{360 Cr \kappa (d^2 - \mu) + Bo d^3 \alpha^2 (5 \kappa - 3 d^2)} . \quad (5)$$

Important information can be extracted from expressions (4) and (5). First of all, these relations can be used to estimate the location of the Marangoni number discontinuity in the limit of long wavelengths. This was done by Colinet et al., 2001 for the prescribed temperature case (4) and they obtained

$$\alpha_{d1} \simeq \sqrt{120 \frac{Cr \kappa (1 + d) (\mu - d^2)}{Bo d^3 (\kappa - d^2)}} , \quad (6)$$

whereas for the prescribed heat flux case (5) we obtain

$$\alpha_{d1} \simeq \sqrt{120 \frac{Cr \kappa (\mu - d^2)}{Bo d^3 (5 \kappa / 3 - d^2)}} . \quad (7)$$

Because the Bénard-Marangoni convection is absolutely unstable, the wavenumber in a linear stability analysis has to be a real number. This way, expression (6) is only valid if $d^2 < \mu, \kappa$ or $d^2 > \mu, \kappa$. Similarly, expression (7) is only valid if $d^2 < \mu, 5\kappa/3$ or $d^2 > \mu, 5\kappa/3$. As mentioned before, a further constraint for both estimates (6) and (7) is that α_{d1} has to be a small number. It is interesting to note that when these conditions are not met, as is seen in the next sections, no discontinuity is present in the long wavelength region.

The second important fact extracted from expressions (4) and (5) is that in the limit of zero Crispation number there is another critical depth ratio, given by $d_{c2} = \sqrt{\kappa}$ for the prescribed temperature case (Simanovskii and Nepomnyashchy, 1993) and by $d_{c2} = \sqrt{5\kappa/3}$ for the prescribed heat flux case. When the Crispation number is nonzero, an approximation of order $O(Cr/\alpha^2 Bo)$ for these critical depths can be obtained from expressions (4) and (5). For the prescribed temperature case we find

$$d_{c2} \simeq \sqrt{\kappa + \frac{120}{\alpha_{d2}^2} \left(\frac{1 + \sqrt{\kappa}}{\sqrt{\kappa}} \right) \frac{Cr}{Bo} (\kappa - \mu)} \simeq \kappa^{1/2} \left\{ 1 + \frac{60}{\alpha_{d2}^2} \left(\frac{1 + \sqrt{\kappa}}{\sqrt{\kappa}} \right) \left(1 - \frac{\mu}{\kappa} \right) \frac{Cr}{Bo} \right\}, \quad (8)$$

and for the prescribed heat flux case we find

$$d_{c2} \simeq \sqrt{\frac{5\kappa}{3} + \frac{72}{\alpha_{d2}^2} \sqrt{\frac{3}{5\kappa}} \frac{Cr}{Bo} \left(\frac{5\kappa}{3} - \mu \right)} \simeq \left(\frac{5\kappa}{3} \right)^{1/2} \left\{ 1 + \frac{36}{\alpha_{d2}^2} \sqrt{\frac{3}{5\kappa}} \left(1 - \frac{\mu}{5\kappa/3} \right) \frac{Cr}{Bo} \right\}. \quad (9)$$

where α_{d2} is the wavenumber at which the second discontinuity first appears. It is important to emphasize that, as shown in the next sections, the second discontinuity is never present alone and is always accompanied by the other discontinuity at α_{d1} . Also, α_{d2} cannot be predicted on the basis of either equation (4) or equation (5), and higher order terms are necessary for its estimation.

In general, the parameter $Cr/\alpha^2 Bo$ is a small number and the expressions for the second critical depth ratio d_{c2} obtained in the limit $Cr \rightarrow 0$ are good approximations for small Crispation number cases. Nevertheless, expressions (8) and (9) provide information on how d_{c2} behaves with respect to several different parameters.

All analytical expressions presented so far pertain to the stationary onset of convection. The analytical expressions related to the marginal Marangoni number for an oscillatory onset of convection could not be simplified to anything with a treatable size by the authors and are not shown here. However, numerical results related to this onset of convection are also discussed in the next sections.

In the following sections, the behavior of the marginal Marangoni number is studied and the main control parameter used is the depth ratio between the two fluid layers. In order to facilitate our analysis, a few selected fluids are chosen to be studied and their properties are shown in Tab. (1). It is also important to note that, in the prescribed temperature case, a negative Marangoni number (or temperature difference) represents an onset of instability with the upper wall temperature being higher than the lower wall one. The opposite is true for a positive Marangoni number (or temperature difference). In the prescribed heat flux case, a negative Marangoni number (or heat flux) represents cooling from below whereas a positive Marangoni number (or heat flux) represents heating from below.

Table 1: Properties of Air, Water, n-Hexane and Acetonitrile at $T_0 = 25^\circ C$

	$\mu(m^2/s)$	$k(W/mK)$	$\kappa(m^2/s)$	$\rho(Kg/m^3)$	$\alpha(1/K)$	$\sigma_0(N/m)^*$	$\sigma_T(N/mK)^*$
Air	$1.838 \cdot 10^{-5}$	$2.664 \cdot 10^{-2}$	$2.229 \cdot 10^{-5}$	1.188	$3.271 \cdot 10^{-3}$	—	—
Water	$9.136 \cdot 10^{-4}$	$6.069 \cdot 10^{-1}$	$1.456 \cdot 10^{-7}$	997	$2.635 \cdot 10^{-4}$	$7.213 \cdot 10^{-2}$	$1.774 \cdot 10^{-4}$
n-Hexane	$2.999 \cdot 10^{-4}$	$1.200 \cdot 10^{-1}$	$8.071 \cdot 10^{-8}$	655	$1.41 \cdot 10^{-3}$	$1.789 \cdot 10^{-2}$	$1.022 \cdot 10^{-4}$
Acetonitrile	$3.694 \cdot 10^{-4}$	$1.880 \cdot 10^{-1}$	$1.086 \cdot 10^{-7}$	776	$1.41 \cdot 10^{-3}$	$2.866 \cdot 10^{-2}$	$1.263 \cdot 10^{-4}$

* with respect to air

4. Gas-Liquid Layers

We consider here the case of air above water as being representative of a gas-liquid system, for which the property ratios are: $\mu = 0.02012$, $k = 0.0439$, $\kappa = 153.1$ and $\rho = 0.001192$ (from Tab. (1)).

The behavior of the Marangoni number at the onset of stationary convection in a two-layer system is well known for gas-liquid layers subjected to prescribed temperature boundary conditions (Simanovskii and Nepomnyashchy, 1993). This behavior is shown in Fig. (1), which also shows the corresponding results for the prescribed heat flux boundary condition case. In this figure, the thickness of the lower layer is set to be $d_1 = 0.5 \text{ mm}$, yielding $Cr = 3.689 \cdot 10^{-6}$ and $Bo = 3.38 \cdot 10^{-2}$. Also, dimensional temperature differences and heat fluxes are presented instead of neutral Marangoni numbers Ma_n in order to provide estimates of typical values that would be used in an experiment. For each boundary condition case, results pertaining to three different models are shown in this figure: 1) our two-layer model (solid lines), 2) a ‘‘conducting air-layer’’ model that neglects convection in the upper gas layer (dotted lines with stars, Pérez-García et al., 1998) and 3) the traditional one-layer model in which the dynamics of the gas layer is modelled solely by the Biot number (dashed-dotted lines with squares, Gousbet et al., 1990). The stable range is always within $0 < Ma < |Ma_n|$.

The one-layer model predicts accurate enough results in the short wavelength range ($\alpha > 0.75$) but cannot capture the long wavelength behavior well as seen in Fig. (1). As was mentioned before, this model is not able to capture the discontinuities that can occur in the Marangoni number behavior. Hence, it is valid only when $d_{c1} < d < d_{c2}$. These results were obtained with a small but finite Biot number ($Bi = 10^{-3}$) but the model is actually rather insensitive to small variations in this parameter. The qualitative behavior of the Marangoni number is the same as long as the Biot number has a nonzero value.

Figure (1) also shows results generated from the “conducting air-layer” model, which is obtained from our two-layer solution in the limit of zero dynamic viscosity ($\mu \rightarrow 0$) and zero density ratio ($\rho \rightarrow 0$). This model is much more accurate than the one-layer model and the agreement with our solution is very good as long as $d \gg d_{c1}$. The model is able to capture the discontinuity associated with d_{c2} , since it accounts for the thermal diffusivity of the air-layer, but it cannot capture the discontinuity associated with d_{c1} , since it neglects the viscous effects of the air-layer.

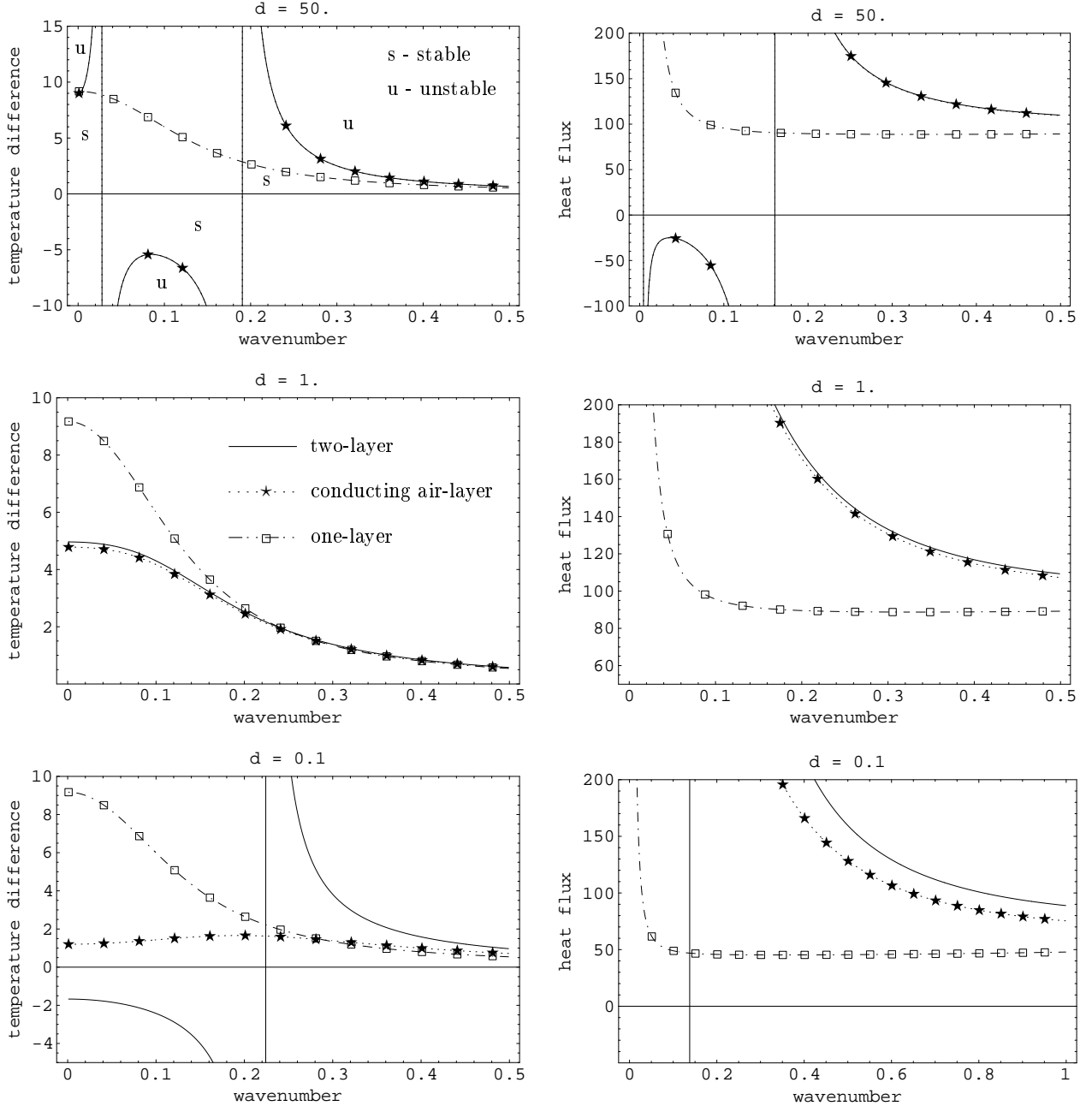


Figure 1: Marginal stability curves for air over water with prescribed temperature (left, ΔT in $^{\circ}K$) and heat flux (right, Q'' in W/m^2) at the bottom rigid surface for $Cr = 3.689 \cdot 10^{-6}$ and $Bo = 3.38 \cdot 10^{-2}$ ($d_1 = 0.5 \text{ mm}$). Vertical solid lines represent the location of the Marangoni number discontinuity in wavenumber space.

The first critical depth ratio predicted by our analysis is an exact result and yields $d_{c1} \simeq 0.136$, for both boundary condition cases. This value is in perfect agreement with the one obtained by numerically examining the full solution for the marginal Marangoni number given by Smith, 1966 for the prescribed temperature case and by equation (1) for the prescribed heat flux case. The second critical depth ratio is an approximate result and yields for a prescribed temperature and heat flux boundary conditions $d_{c2} \simeq 12.1$ and 14.1 , respectively. The values obtained from the full solution for the marginal Marangoni number are $d_{c2} \simeq 12.8$ and 14.5 .

Critical Marangoni numbers Ma_c and wavenumbers α_c for the case of air over a water layer with $d_1 = 1\text{ mm}$, which yields $Cr = 1.844 \cdot 10^{-6}$ and $Bo = 0.1354$, are shown in Fig. (2) as functions of the depth ratio. Like before, the stable range is always within $0 < Ma < |Ma_c|$. One important characteristic that can be noticed in this figure is that prescribing a heat flux instead of a temperature at the lower boundary reduces the numerical value of the critical Marangoni number for both heat transfer from above and below, but specially from above.

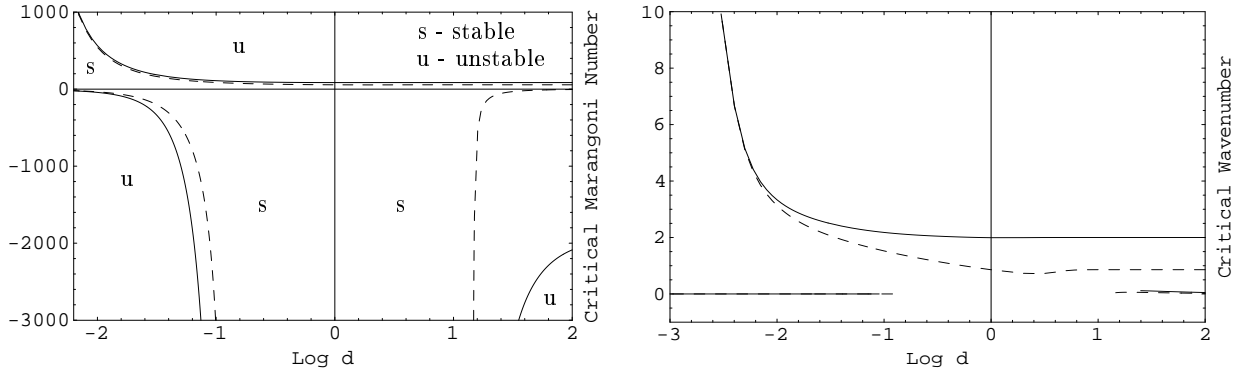


Figure 2: Critical Marangoni number vs and wavenumber as functions of the depth ratio for $Cr = 1.844 \cdot 10^{-6}$ and $Bo = 1.354 \cdot 10^{-1}$ ($d_1 = 1\text{ mm}$). Prescribed temperature case given by solid lines and prescribed heat flux case given by dashed lines.

It has been noted previously (Velarde et al., 2001) that an oscillatory onset of convection is not realizable for an air-water system because the critical Marangoni number associated with it is always higher than the one obtained for a stationary onset, for cases of heat being transferred either from above or below. By examining Fig. (1), one might think that an oscillatory onset of convection is possible for the case of heat being transferred from above when $d_{c1} < d < d_{c2}$ since, within this range of depth ratios, a stationary onset of convection is suppressed. However, an oscillatory onset of convection cannot be achieved because the temperature differences or heat fluxes needed are too high (Regnier et al., 2000 and Juel et al., 2000).

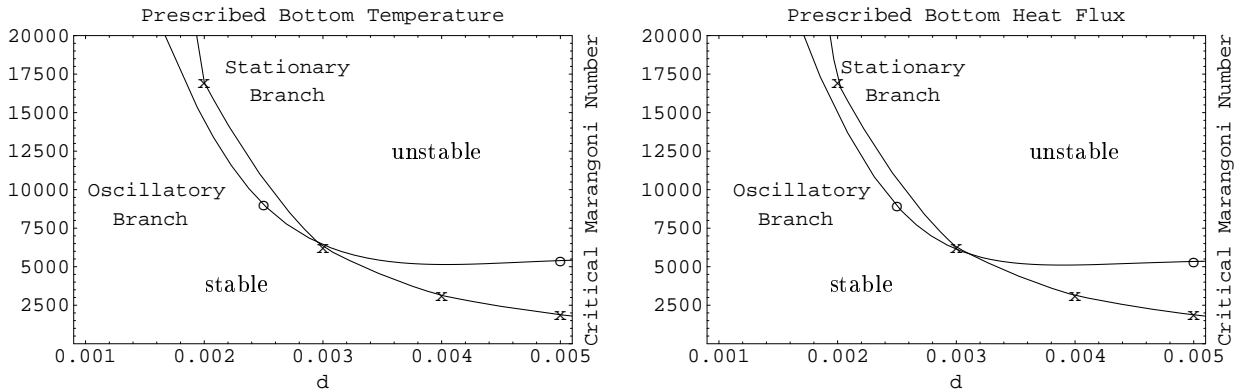


Figure 3: Critical Marangoni number as a function of the depth ratio for prescribed temperature ($\alpha_{e,stat.} \simeq 10.17$, $\alpha_{e,osc.} \simeq 2.3$, $\omega_e \simeq 42.12$) and heat flux cases ($\alpha_{e,stat.} \simeq 9.46$, $\alpha_{e,osc.} \simeq 2.21$, $\omega_e \simeq 40.49$) for air over water with $d_1 = 1\text{ mm}$ ($Cr = 1.844 \cdot 10^{-6}$ and $Bo = 1.354 \cdot 10^{-1}$).

Nonetheless, Slavtchev et al., 1998 have found that a constant heat flux boundary condition can promote oscillatory instability when studying the one-layer model. However, this was only achieved at relatively high Crispation numbers ($Cr > 0.006$). In general, such high values of this parameter can be obtained by decreasing the thickness of the liquid layer to very small values. We have investigated numerically such a feature using our two-layer model and found interesting results. As one can see in Fig. (1), the large wavelength instability due to heat transfer from below is suppressed when the depth ratio is decreased below d_{c1} since the fluid is only unstable to heat being transferred from above in this region. As the depth ratio is further decreased, not only does the $Ma < 0$ region increase but also does the critical Marangoni number for the stationary onset of convection. At the same time, we have found that the critical Marangoni number for the oscillatory onset of convection decreases, reaches a minimum and then starts increasing again, but at a rate lower than the critical value for the stationary onset. This trend is shown in Fig. (3), where the exchange of instability onsets occurs at $d_e \simeq 2.96 \cdot 10^{-3}$ and $Ma_e \simeq 6585$ (or $\Delta T \simeq 4.94\text{ K}$) for the prescribed temperature case, and $d_e \simeq 3.12 \cdot 10^{-3}$ and $Ma_e \simeq 5810$ (or $q_s \simeq 2.65\text{ kW/m}^2$) for the prescribed heat flux case. Although the exchange point is

relatively insensitive to the choice of thermal boundary condition, the oscillatory instability has significantly larger wavelengths than the stationary instability. A drawback that might not allow this result to be verified experimentally is the very low value of the air-layer thickness, which could make the unevenness of the upper solid wall an important parameter. This problem may be avoided by increasing the thickness of the liquid layer, but this was not attempted here since buoyancy effects, not included in our model, might then become important.

5. Liquid-Liquid Layers

The impact of imposing a prescribed heat flux boundary condition on a liquid-liquid system is analyzed through the consideration of an n-hexane liquid phase over an acetonitrile one. We made this choice of liquids because an oscillatory onset of convection was observed in the experiment reported by Juel et al., 2000 in which these liquids were used.

The properties of these liquids are presented in Tab. (1), for a reference temperature $T_0 = 25^\circ\text{C}$, where the surface tension values shown are with respect to air. Both surface tension coefficients σ_0 and σ_T between liquids could be estimated from the ones given in Tab. (1) using Antonow's rule but the values given by Juel et al., 2000 are used instead. From this table, we are able to obtain the following property ratios: $\mu = 0.8119$, $k = 0.6383$, $\kappa = 0.7432$ and $\rho = 0.8441$.

For gas-liquid systems in general, we have $d_{c2} > d_{c1}$ independently of the boundary condition prescribed. This allows us to set these critical depth ratios as bounds for the applicability of the one-layer model. However, such a characteristic doesn't necessarily carry on for a two-liquid system. In fact, an interesting feature appears for our choice of liquids. This choice leads to $d_{c1} \simeq 0.901$ and either $d_{c2} \simeq 0.859$ ($d_{c1} > d_{c2}$) for the prescribed temperature case or $d_{c2} \simeq 1.113$ ($d_{c2} > d_{c1}$) for the prescribed heat flux case. These results for d_{c2} are based on $d_1 = 1\text{ mm}$, which yields $Cr = 3.726 \cdot 10^{-6}$ and $Bo = 0.111$. It is interesting to note that our definition of dimensionless parameters gives $Cr/Bo \sim d_1^{-3}$. Hence, equation (8) indicates that if d_1 is decreased the value of d_{c2} for the prescribed temperature case decreases because $\mu > \kappa$. However, equation (9) indicates that if d_1 is decreased the value of d_{c2} for the prescribed heat flux case increases because $\mu < 5\kappa/3$.

The behavior of the marginal Marangoni number as a function of the wavenumber for different depth ratio values is shown in Fig. (4) for $d_1 = 1\text{ mm}$. In this figure, the prescribed temperature case is shown on the left whereas the prescribed heat flux case is shown on the right. First, we focus our discussion on the prescribed temperature case. As long as $d > d_{c1}$, the discontinuity is located in the long wavelength region and the marginal Marangoni number is positive there. By limiting the depth ratio to the range $d_{c1} > d > d_{c2}$, the discontinuity disappears and the fluid is unstable to heat being transferred from above only. As the depth ratio d is decreased to d_{c2} , a discontinuity at a finite nonzero wavenumber appears. As the depth ratio is further decreased, this discontinuity bifurcates into two discontinuities that create a positive Marangoni number region between negative Marangoni number regions. This positive region increases in size as the depth ratio is further decreased.

As mentioned before, by prescribing the heat flux instead of the temperature at the lower wall we obtain $d_{c2} > d_{c1}$. However, approximate expressions were used to generate this result. The marginal Marangoni number behavior as obtained from the full solution (1) for the prescribed heat flux case is also shown in Fig. (4). It turns out that, unlike the prescribed temperature case, the Marangoni number has a discontinuous behavior for any value of the depth ratio. The reason for this discrepancy is that α_{d2} is actually zero and not a finite nonzero number as in the prescribed temperature case. Hence, according to equation (9), $d_{c2} \rightarrow \infty$ and becomes meaningless. This way, as long as $d > d_{c1}$, the marginal Marangoni number is positive within the long wavelength region and negative elsewhere. As the depth ratio is further decreased and $d < d_{c1}$, the Marangoni number behavior is similar for both prescribed boundary condition cases.

Critical Marangoni numbers, wavenumbers and frequencies as functions of the depth ratio are shown in Fig. (5). Solid lines represent the prescribed temperature case whereas dashed lines represent the prescribed heat flux case. Also, stationary onsets of convection are shown without symbols whereas oscillatory ones are shown with symbols. These results are based on $d_1 = 1\text{ mm}$. One can see in this figure that the critical Marangoni number for a stationary onset of convection due to heat transfer from below is decreased by imposing a heat flux at the bottom rigid boundary. The changes are not as significant when heat is being transferred from above. In contrast to the gas-liquid case, we could not find an oscillatory instability in the limit of very low depth ratios. However, oscillatory onset of convection can be achieved for the two-liquid system at higher depth ratios, e.g. $d > 1$, as predicted and observed in the work of Juel et al., 2000. One can also see in this figure that critical Marangoni numbers for an oscillatory onset of convection can be decreased by prescribing the heat flux instead of the temperature at the bottom rigid boundary. Results for $d > 2$ are not analyzed because buoyancy effects would have to be considered. We also note here that, although not shown in this figure, stationary and oscillatory curves for the critical Marangoni number do intersect at around $d \simeq 1$. Finally, by comparing the long wavelength results by Juel et al., 2000 to ours, we note that they agree well in the limit of low depth ratios. This leads to the conclusion that buoyancy forces are negligible in the long wavelength range.

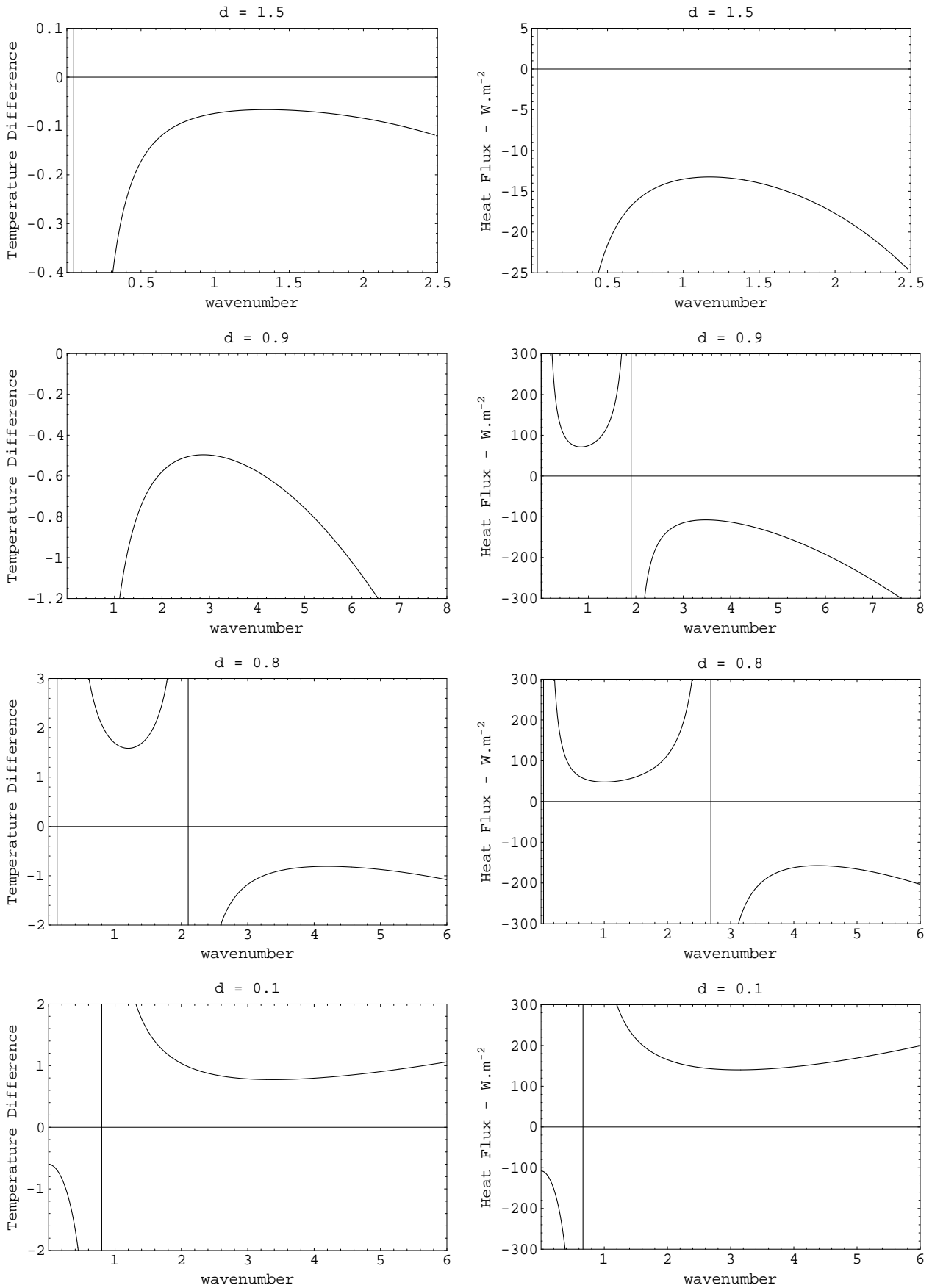


Figure 4: Marginal stability curves for n-hexane over acetonitrile for prescribed temperature (ΔT in $^{\circ}K$) and heat flux (Q'' in W/m^2) at the bottom rigid surface for $Cr = 3.726 \cdot 10^{-6}$ and $Bo = 1.11 \cdot 10^{-1}$ ($d_1 = 1 mm$). Vertical solid lines represent the location of the Marangoni number discontinuity in wavenumber space. Stable and unstable regions defined as in figure 1 (stable within $0 < Ma < |Ma_n|$, unstable otherwise).

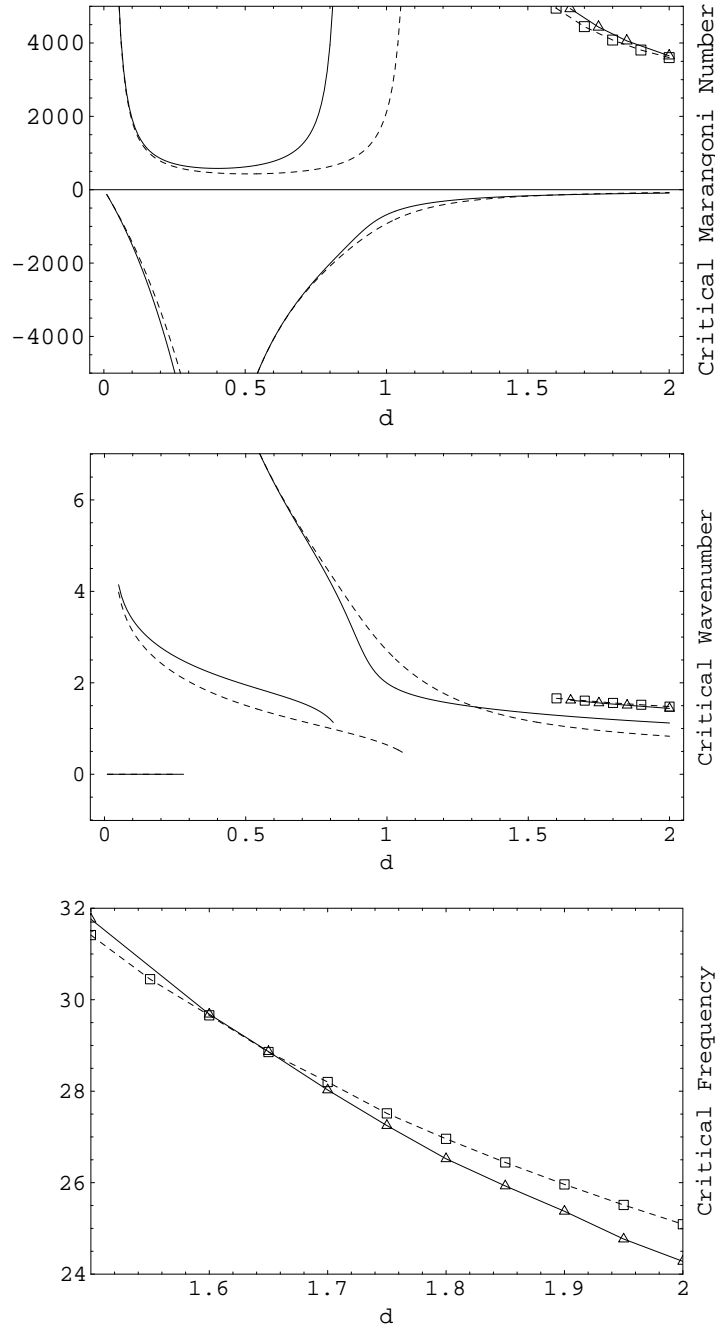


Figure 5: Comparison between critical Marangoni number, wavenumber and frequency as functions of the depth ratio for the prescribed temperature (solid lines) and prescribed heat flux (dashed lines) cases for stationary (no symbols) and oscillatory (symbols) onset of convection with $Cr = 3.726 \cdot 10^{-6}$ and $Bo = 1.11 \cdot 10^{-1}$ ($d_1 = 1 \text{ mm}$). Stable and unstable regions defined as in figure 2 (stable within $0 < Ma < |Ma_c|$, unstable otherwise).

6. Conclusions

The *Mathematica* software proved to be very efficient from beginning to end due to its analytical, numerical and graphical resources. Its symbolic computation capabilities simplified greatly all analytical derivations and allowed us to explore in depth the physical trends of the problem at hand.

The impact of using a prescribed heat flux boundary condition instead of a temperature one was demonstrated. This change decreased the critical Marangoni number for heat transfer from either direction in an air-water system, and for heat transfer from below in a n-hexane-acetonitrile liquid system. Also, oscillatory onset of convection was shown to be possible for an air-liquid system for very low depth ratio values. This unstable convection mode was also shown to be possible for an n-hexane liquid layer over an acetonitrile liquid layer as long as $d > 1$.

7. Acknowledgements

Leonardo Alves wishes to express his gratitude to the UCLA Academic Senate and to the Brazilian governmental sponsor agency CAPES for their financial support.

8. References

- Bénard, H., 1900, Les Tourbillons Cellulaires dans une Nappe Liquide, “Rev. Gén. Sci. Pures Appl.”, Vol. 12, pp. 1261–1309.
- Block, M., 1956, Surface Tension as the Cause of Bénard Cells and Surface Deformation in a Liquid Film, “Nature”, Vol. 178, pp. 650.
- Colinet, P., Legros, J. C., and Velarde, M. G., 2001, “Nonlinear Dynamics of Surface-Tension-Driven Instabilities”, Wiley-VCH Verlag, Berlin.
- Gousbet, G., Maquet, J., Roze, C., and Darrigo, R., 1990, Surface-Tension and Couple Buoyancy-Driven Instability in a Horizontal Liquid Layer: Overstability and Exchange of Stability, “Physics of Fluids”, Vol. 2, No. 6, pp. 903–911.
- Hondros, E. D., Mclean, M., and Mills, K. C., 1998, Marangoni and Interfacial Phenomena in Material Processing, “Philosophical Transactions of the Royal Society of London”, A-356, p. 811.
- Jiménez-Fernández, J. and García-Sanz, J., 1996, Marangoni Oscillatory Instabilities in Two-Layer Systems, “Microgravity Science and Technology”, Vol. IX, No. 4, pp. 245–256.
- Johnson, D. and Narayanan, R., 1999, A Tutorial on Rayleigh-Bénard-Marangoni Problem with Multiple Layers and Side Wall Effects, “Chaos”, Vol. 9, No. 1, pp. 124–140.
- Juel, A., Burgess, J. M., McCormick, W. D., Swift, J. B., and Swinney, H. L., 2000, Surface Tension-Driven Convection Patterns in Two Liquid Layers, “Physica D”, Vol. 143, pp. 169–186.
- Kuhlmann, H. C., 1999, “Thermocapillary Convection in Models of Crystal Growth”, Springer Verlag.
- Narayanan, R. and Schwabe, D., editors, 2003, “Interfacial Fluid Dynamics and Transport Processes”, Springer Verlag.
- Nepomnyashchy, A. A., Velarde, M. G., and Colinet, P., 2001, “Interfacial Phenomena and Convection”, Vol. 124 of “Monographs and Surveys in Pure and Applied Mathematics”, Chapman & Hall/CRC, Boca Raton.
- Or, A. C. and Kelly, R. E., 2001, Feedback control of weakly nonlinear Rayleigh-Bénard-Marangoni Convection, “Journal of Fluid Mechanics”, Vol. 440, pp. 27–47.
- Pearson, J. R. A., 1958, On Convection Cells Induced by Surface Tension, “Journal of Fluid Mechanics”, Vol. 4, pp. 489–500.
- Pérez-García, C., Echebarria, B., and Bestehorn, M., 1998, Thermal Properties in Surface-Tension-Driven Convection, “Physical Review E”, Vol. 57, No. 1, pp. 475–481.
- Regnier, V. C., Dauby, P. C., and Lebon, G., 2000, Linear and Nonlinear Rayleigh-Bénard-Marangoni Instability with Surface Deformations, “Physics of Fluids”, Vol. 12, No. 11, pp. 2787–2799.
- Simanovskii, I., Georis, P., Nepomnyashchy, A., and Legros, J. C., 2003, Oscillatory Instability in Multilayer Systems, “Physics of Fluids”, Vol. 15, pp. 3867.
- Simanovskii, I. B. and Nepomnyashchy, A. A., 1993, “Convective Instabilities in Systems with Interface”, Gordon and Breach Science Publishers S.A., Amsterdam.
- Slavtchev, S. G., Kalitzova-Kurteva, P. G., and Kurtev, I. A., 1998, Oscillatory Marangoni Instability in a Liquid Layer with Temperature-Dependent Viscosity and Deformable Free Surface, “Microgravity Science and Technology”, Vol. 11, pp. 29–34.
- Smith, K. A., 1966, On Convective Instability Induced by Surface-Tension Gradients, “Journal of Fluid Mechanics”, Vol. 24, pp. 401–414.
- Takashima, M., 1981a, Surface Tension Driven Instability in a Horizontal Liquid Layer with a Deformable Free Surface - I. Stationary Convection, “Journal of the Physical Society of Japan”, Vol. 50, No. 8, pp. 2745–2750.
- Takashima, M., 1981b, Surface Tension Driven Instability in a Horizontal Liquid Layer with a Deformable Free Surface - II. Overstability, “Journal of the Physical Society of Japan”, Vol. 50, No. 8, pp. 2751–2756.
- Velarde, M. G., Nepomnyashchy, A. A., and Hennenberg, M., 2001, Onset of Oscillatory Interfacial Instability and Wave Motions in Bénard Layers, “Advances in Applied Mechanics”, Vol. 37, pp. 167–238.
- Wolfram, S., 1999, “The Mathematica Book”, Wolfram Media, Cambridge, 4th edition.
- Yang, H. Q., 1992, Boundary Effect on the Bénard-Marangoni Instability, “International Journal of Heat and Mass Transfer”, Vol. 35, No. 10, pp. 2413–2420.
- Zaman, A. A. and Narayanan, R., 1996, Interfacial and Buoyancy-Driven Convection - The Effect of Geometry and Comparison with Experiments, “Journal of Colloids and Interface Science”, Vol. 179, pp. 151–162.